Egypt. J. Chem. **Vol. 65,** No. 12 pp. 493 - 508 (2022)

Egyptian Journal of Chemistry

http://ejchem.journals.ekb.eg/

Modulatory Effects of Cilostazol; an Nrf2/HO-1 activator against NAFLD in Rats Confirmed by Molecular Docking and FTIR Studies

Ahmed A. Sedik [1]*, Asmaa A. Amer[2]

[1]*Department of Pharmacology, Medical Research and Clinical Studies Institute, National Research Centre, Dokki, 12622, Cairo, Egypt*

[2]*Department of Pharmacognosy Pharmaceutical and Drug Industries Research Institute, National Research Centre, Dokki, 12622, Cairo, Egypt*

Abstract

Nonalcoholic fatty liver disease (NAFLD) is a multi-etiological hepato-metabolic syndrome. No effective drugs have been settled for the effective therapy of NAFLD. Our study was conducted to evaluate the modulatory effects of cilostazol (CILO, 50 and 100 mg/kg.p.o.) against NAFLD induced by high fat diet rich in cholesterol (HFD- CH) for 10 weeks. Forty male Sprague dawely rats were divided into 4 groups (10 rat / group). Normal control group supplied with normal chow diet. Control positive group received HFD- CH for 10 weeks. In addition, two CILO groups received (CILO, 50 and 100 mg/kg.p.o.) concurrently with HFD-CH. Our findings revealed that CILO at a dose level (100 mg/kg) showed promising results in reducing fasting glucose and insulin levels. Moreover, it could reduce the elevated inflammatory cytokines, hepatic lipids and oxidative stress biomarkers. In addition, CILO succeeded to restore the total protein levels and activate nuclear factor erythroid-related factor2/heme oxygenase-1 (Nrf2/HO-1) activity. Furthermore, administration of CILO for NAFLD rats succeeded to show corrected and normalized FTIR spectra. We also investigated the plausible binding interactions of CILO with various biological targets using a molecular docking approach, and the results showed that CILO had an excellent docking energy score and significant binding interactions with the core amino acids involved in the active pocket for the enzymes studied. This study confirmed that CILO exerted a new intervention for NAFLD due to its complementary anti-hyperlipidemic, anti-inflammatory, and antioxidant potential, which was achieved through Nrf2/HO-1 activation**.**

Keywords: NAFLD, Cilostazol, Nrf2/HO-1, FTIR, molecular docking.

1. Introduction

Nonalcoholic fatty liver disease (NAFLD) has a dramatically rising incidence in the western world and its prevalence continues to increase as a health crisis in society. Hepatic lipid accumulation can triggers hepatocyte damage, inflammation and fibrogenesis **(1)**. NAFLD is strongly associated with the risk of more severe conditions such as atherosclerosis and cardiovascular diseases **(2)**. Liver is the primary modulator of the biological pathways involved in cholesterol synthesis, cholesterol metabolism, uptake from chylomicron remnants, re-uptake from high-density lipoproteins (HDL), cholesterol release from very-low density lipoproteins (VLDL), and biliary acid production. All of these pathways have a dominant effect on the regulation of plasma cholesterol concentrations and, as a result, on the increase of lipoprotein triglyceride (TGS) particles in the blood, resulting in fatty disposition in the peripheral tissues and liver. The most important precipitating factors associated with liver injury are inflammation and oxidative stress **(3)**.

NAFLD induced by high fat diet rich in cholesterol (HFD-CH) was related primarily to an oxidative injury and inflammation **(4)**.Under normal and oxidative conditions, regulation of redox hemostasis occurs chiefly at the nucleus, and the nuclear factor erythroid-related factor2 (Nrf2) / hemoxygenase-1 (HO-1) signalling pathway is an important mediator for modulation of such responses **(5)**. The impairment in the cellular redox homeostasis causes deviation in the level of inflammatory mediators such as nuclear factor kappa-b (NF-κB**)** and tumor necrosis factor (TNF-α) which are required for repairing and regeneration of hepatocytes **(6)**. Therefore, to avoid harmful oxidative conditions and to restore the redox homeostasis, activation of (Nrf2/HO-1) must being achieved **(7)**. Several experimental and clinical attempts have been postulated for the therapy of the NAFLD, but none

*Corresponding author e-mail: aa.sedik@gmail.com.; (Ahmed A. Sedik).
Receive Date: 15 May 2022, Revise Date: 07 June 2022, Accept Date: 16 June 2022
DOI: 10.21608/EJCHEM.2022.138491.6091

have shown prominent results on liver biomarkers and hepatic regeneration **(8)**. Thus, there is a pressing need to find safe therapeutic medicines that can alleviate the precipitating factors and diminish the hepatic accumulation of fats surrounding the liver.

Cilostazol (CILO) is a promising research topic because of its significant results in reducing reactive oxygen species (ROS) by acting as a non-enzymatic antioxidant in reducing ROS **(9)**. CILO is a quinolone derivative approved from FDA in the treatment of intermittent claudication due to peripheral vascular disease **(10)**. It was also used principally in treatment of thrombotic diseases due to its anti-platelet activates. It also reduces the generation of intracellular ROS, which suppresses apoptosis and inflammatory alterations in several animal models **(11)**.

Molecular Docking is a theoretical technique used to investigate protein-ligand interactions and recognition. Small molecule ligands are studied in their interactions with receptor bio-macromolecules to determine the degree of binding and the strong of their affinity. These interactions are then used for developing structure-based drug design in order to study the molecular mechanisms of the pharmacological effects, predicting the structure of protein or ligand–ligand complexes, and enabling targeted drug discovery **(12)**. The increasing computing power and improved insights from computational chemistry approaches, as well as the transformative impact of applying machine learning models to chemical sciences **(13)**.

Therefore, this study was conducted to assess the possible modulatory effects of cilostazol against metabolic, biochemical, and molecular alterations induced by high-fat, high-cholesterol diet (HFD- CH) that mimics the pathophysiological features of NAFLD in humans. Molecular docking studies can help predict which compounds have the highest active potential against NAFLD proteins.

2. Materials and Methods

2.1. Laboratory animals

Forty male Sprague dawely rats weighing 120-150 g were used throughout the study. Rats were acclimated to the animal research colony's ideal environmental laboratory settings (National Research Centre, Cairo, Egypt). Rats were fed a typical laboratory meal ad libitum with unlimited access to water. The study was carried out in compliance with the Medical Research Ethics Committee (MREC) of the National Research Centre in Dokki, Egypt's ethical norms (No.13111).

2.2. Induction of NAFLD

NAFLD was induced by daily intake from high fat diet rich in cholesterol (HFD-CH) composed of fat (55%), cholesterol powder (4%) , carbohydrate (20%) and protein (21 %), with equal quantities of minerals, vitamins and fibers **(14)**. Cilostazol and cholesterol powder were purchased from sigma-Aldrich (USA).In addition, kits and chemicals were supplied from Randox.co, UK.

2.3. Experimental design

Forty male sprague dawely rats, were divided into 4 groups (10 rats / group). Normal control group supplied with normal chow diet. Control positive group received HFD-CH for 10 weeks. In addition to, two CILO groups received (CILO,50 and 100 mg/ kg.p.o.) concurrently with HFD-CH **(15)**. At the end of the experiment, rats were starved overnight, and blood samples were taken from the retro-orbital plexus of ether-anesthetized animals and centrifuged (800g, 4°C, 20 min.) to separate serum, which was then tested for metabolic and biochemical indices.

Rats were sacrificed and liver tissues were excised, homogenized and divided into two parts. Part one is centrifuged at 4°C (4000 rpm/min., 5 min.), and the supernatants were analyzed for determination of hepatic concentration of further biochemical indices. Part two is freeze dried and prepared for investigation of molecular alterations by the aid of fourier transform infrared (FTIR) spectroscopy.

2.3.1. Metabolic and biochemical assessment

The concentration of fasting serum glucose was measured using glucose oxidase method, colorimetrically at 505 nm **(16)**. Serum insulin level was determined by enzyme immunoassay kit **(17)**. Serum levels of aspartate aminotransferase (AST), alanine aminotransferase (ALT) were measured colorimetrically at 510 nm **(18)**. Similarly, hepatic levels of total cholesterol (TC) and triglycerides (TG) were estimated at 505 nm using a calorimetric kit. In addition , serum lipids and total proteins were evaluated **(19, 20).**

2.3.2. Assessment of GSH and MDA levels in hepatic homogenate

The hepatic concentration of reduced glutathione (GSH) was assessed depending on a colorimetric reaction where reduction of 5, 5-dithiobis-(2-nitrobenzoic acid) (DTNB) by SH group of glutathione occurs forming 2-nitro-S-

mercaptobenzoic acid. The forming product was measured spectrophotometrically at 412 nm **(21)**. In addition, the hepatic content of lipid peroxidation product, expressed as malondialdehyde (MDA) was determined through a reduction reaction occurs between one molecule of malondialdehyde with two molecules of 2-thiobarbituricacid under optimal conditions at pH, 3.5) forming pink coloured product that can be detected spectrophotometrically at 532 nm **(22)**.

2.3.3. Assessment of NO, SOD and HO-1 levels in hepatic homogenate

Nitric oxide (NO) concentration was measured in liver homogenate via griess reaction , that involved in reduction of nitrate to nitrite, where the mixture of naphthylethylenediamine and sulfanilamide was estimated spectrophotometrically at 540 nm **(23)**. Superoxide dismutase (SOD) activity was measured in liver homogenate at 420 nm by a spectrophotometer using colorimetric kit **(24)**. Hepatic heme oxygenase-1 (HO-1) concentration was determined by spectrophotometry at 450 nm using the Eliza kit, and HO-1 concentration was reported as ng/mg tissue **(25)**.

2.3.4. Fourier transform infrared spectroscopy (FTIR) spectra in hepatic tissue

FTIR spectroscopy is a reliable and non-invasive method that can provide a clear picture of macromolecule functional and structural changes within tissue cells **(26).** Hepatic tissue samples were lyophilized for 24 h then an equal and small amount of dried liver tissue samples were gently mixed with potassium bromide (KBr) crystals under a suitable pressure (1200 psi) for eight minutes to produce KBr pellets. In order to gain the same thickness of each pellet, samples were weighted and subjected to the same pressure. Pellets were scanned at 4 cm-1 within the mid-IR spectra (3200–400 cm-1) at room temperature and the spectra was recorded using a Perkin Elmer Spectrum (Perkin Elmer Inc, USA) equipped with a DTGS detector **(27).**

2.4. Statistical analysis

One-way ANOVA were used for all statistical comparisons performed followed by Tukey's multiple comparison test, and the results are expressed as mean ± SEM (8 rats). Graph Pad Prism version no. 8.0. (GraphPad Software, Inc., CA, USA) was used for the data examination. The difference is considered significant when the *p* value is less than 0.05.

2.5. Computational analysis

The crystal structures of target proteins were obtained using codes from the protein data bank at http://www.rscb.org/pdb. as illustrated in **Table 1(28-35)**. The water molecules were removed and the enzymes were prepared using QuickPrep tool module in MOE 2019.01 (Molecular Operating Environment, Version 2019.01, Chemical Computing Group Inc., Montreal, Canada), then active site was identified.

The chemical structure of CILO was obtained from PubChem (https://pubchem.ncbi.nlm.nih.gov/) as sdf files then loaded to MOE program. The structures were minimized using the MMFF94x force field until the RMSD of 0.01 kcal mol^{-1} $Å^{-1}$was reached. The induced-fit protocol was used in the docking simulation, with the Triangle Matcher method used to place ligand conformations in the site, which were then ranked using the London ΔG scoring function. The docking protocol was validated by running docking for the target protein's co-crystallized ligands. All the re-docked ligands had a low RMSD value less than 2 $Å^{-1}$, indicating that the docking protocol was valid. One hundred docking poses were calculated, and the resulting docking poses were visualized using MOE 2019.01. The top-scored docking poses were used to calculate the binding free energy (ΔG) of CILO in kcal/mol.

Table 1: Binding affinity and interaction of cilostazol with the target proteins.

Protein	PDB code	Binding energy (kcal/mol)	Type of interaction, distance (Å)	cilostazol atoms involved in the interaction	Amino acid involved in the interaction
PPAR-γ	**3K8S**	-8.86	Two H-donor, 3.49 & 3.66	NH	MET 348
			H-acceptor, 3.42	N of tetrazole ring	GLN 286
			Three pi-H, 3.70, 3.75 & 3.84	Tetrazole ring	CYS 285, HIS 449
PPAR-α	**3ET1**	-9.39	Two H-acceptor, 3.28, 3.28	C=O	TYR 334
HO-1	**1DVE**	-8.06	two H-acceptor, 3.37 Pi-cation, 3.32	N of tetrazole ring Tetrazole ring	ASP 140 ARG 136

Nrf-2	**5CGJ**	-8.06	two H-acceptor, 3.11, 2.98	C=O	ARG 483
TNF-α	**2AZ5**	-6.39	four H-donor, 3.29	NH and N of tetrazole ring	GLY 121
			two pi-H, 4.20, 4.25	Tetrazole ring	LEU 55
GSH	**1XAN**	-6.57	three H-acceptor, 3.02	C=O	SER 470
			three H-acceptor, 3.27, 3.36	N of tetrazole ring	HIS 82
iNOS	**4CX7**	-7.60	three H-donor , 3.65, 3.64, 43.65	NH	MET 355
			three H-donor, 4.21, 4.04, 4.16	Cyclohexane ring	CYS 200
			five H-acceptor, 3.05, 2.84, 2.89	CO	TYR 491
			Two H-acceptor, 3.04, 3.09	N of tetrazole ring	SER 242
			Two pi-H, 3.30	tetrazole ring	GLY 371
			Three six pi-H, 4.52	tetrazole ring	GLY 202
Catalase	**1TGU**	-9.55	Three H-acceptor, 2.72, 2.85, 2.88	N of tetrazole ring	ARG 364
			Three pi-pi, 3.73, 3.56, 3.77	Phenyl ring	PHE 160

3. RESULTS

3.1. Effect of CILO on the serum levels of glucose, insulin, total lipids and total proteins in NAFLD rats

Adding high fat diet rich in cholesterol to rats for 10 consecutive weeks was associated with an increase in the levels of fasting serum glucose, insulin and total lipids reaching about 171%, 147% and 149%, respectively, compared with normal healthy rats. Oral treatment of rats with CILO (50 mg/kg) for 10 consecutive weeks concurrent with HFD-CH was associated with a decrease in the levels of fasting serum glucose, insulin and total lipids reaching about 73% , 89%, respectively. Administration of CILO (100 mg/kg) for NAFLD rats succeeded to restore the normal fasting glucose, insulin and total lipids levels **(Figure 1).**

Induction of NAFLD in rats by continuous daily consumption of HFD-CH for 10 weeks showed a decrease in total protein levels reaching about 75%, compared with normal control group. Oral treatment of rats with CILO (50 mg/kg) for 10 consecutive weeks concurrent with HFD-CH was associated with an increase in the levels of fasting serum total protein levels reaching about 121%, respectively, compared with HFD-CH received rats. Administration of CILO (100 mg/kg) for NAFLD rats succeeded to restore the fasting normal total protein levels **(Figure 2).**

3.2. Effect of CILO on serum AST, ALT, ALP levels and hepatic concentration of TG_S and TC in NAFLD rats

Adding HFD-CH for 10 consecutive weeks was associated with an elevation in the levels of serum AST, ALT, ALP levels, hepatic concentration of TG_S and TC reaching about 6 folds, 3 folds, 6 folds, 153 % and 235% respectively. Oral treatment of rats with CILO (50 mg/kg) for 10 consecutive weeks concurrent with HFD-CH was associated with a decrease in the levels of serum AST, ALT, ALP levels, hepatic concentration of TG_S reaching about 35%, 50%, 32%, 72% , respectively and normalizing the levels of hepatic TC. Administration of CILO (100 mg/kg) for NAFLD rats succeeded to reduce the levels of serum AST, ALT, ALP levels, hepatic concentration of TG_S reaching about 18%, 25%, 25%, respectively and normalizing the levels of hepatic TG_S and TC **(Table 3).**

3.4. Effect of CILO on hepatic oxidative stress biomarkersin NAFLD rats

NAFLD in rats was induced by continuous daily consumption of HFD-CH for 10 weeks revealed an increase in the concentration of hepatic MDA and NO reaching about 250% and 5 folds . In addition, a decrease in hepatic GSH reaching about 36%, compared with normal control rats. Oral treatment of rats with CILO (50 and 100 mg/kg) for 10 consecutive weeks concurrent with HFD-CH revealed a decrease in the concentration of hepatic MDA and NO reaching about 43% and 32%. In addition, an increase in hepatic GSH reaching about 32%, compared with control positive rats. Oral administration of CILO (100 mg/kg) for NAFLD rats succeeded to normalizing the levels of hepatic GSH, MDA and NO **(Table 4).**

3.5. Effect of CILO on hepatic levels of pro-inflammatory cytokines in NAFLD rats

Adding HFD-CH for 10 consecutive weeks was associated with the elevation in the hepatic levels of TNF-α and NF-κB reaching about 364% and 453%, respectively, compared with NAFLD group. Oral administration of CILO (50 mg/kg) for 10 consecutive weeks concurrent with HFD-CH was associated with a decrease in the hepatic levels of TNF-α and NF-κB reaching about 50% and 29% , respectively, compared with control positive group. Administration of CILO (100 mg/kg) for NAFLD rats succeeded to normalize the hepatic levels of TNF-α and NF-κB **(Table 5).**

3.6. Effect of CILO on hepatic levels of Nrf-2 expression and HO-1 levels in NAFLD rats

Administration of HFD-CH for 10 consecutive weeks for was associated with a decrease in the hepatic levels of Nrf-2 expression and HO-1 reaching about 21% and 40% respectively, compared with NAFLD group. Oral treatment of rats with CILO (50 mg/kg) for 10 consecutive weeks concurrent with HFD-CH was one of the causes of increasing in the hepatic levels of Nrf-2 expression and HO-1 reaching about 180% and normalization of HO-1 expression, respectively, compared with control positive group. Administration of CILO (100 mg/kg) for NAFLD rats succeeded to normalize the hepatic levels of Nrf-2 expression and HO-1 activity **(Figure3).**

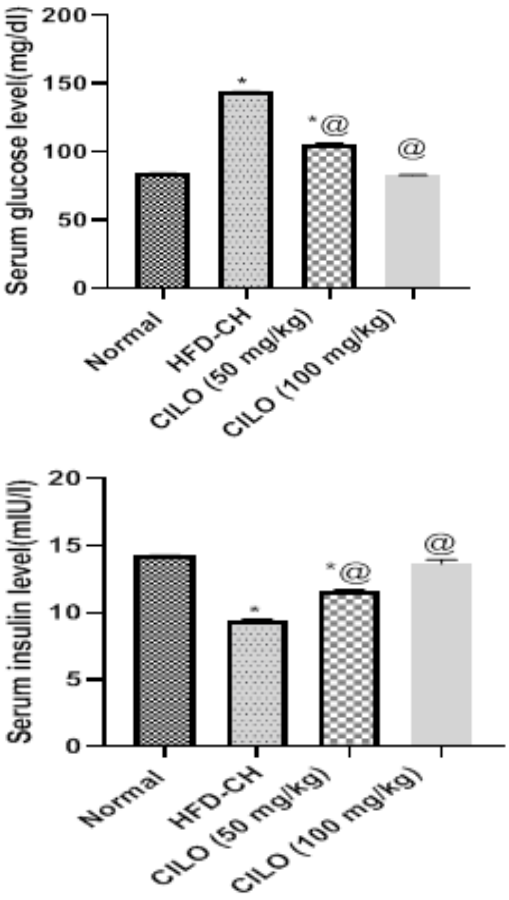

NAFLD was induced by daily administration of high fat diet rich in cholesterol for 10 weeks. Oral treatment of HFD-CH induced- NAFLD with CILO (50 and 100 mg/kg). 24 hours after the last dose of the drugs, fasting serum glucose and insulin levels were evaluated. Results are expressed as mean ±SEM (n=8). *Significant difference from normal control group p< 0.05. @ Significant difference from NAFLD group.

Figure.1. Effect of cilostazol on fasting serum glucose and insulin levels of NAFLD rats

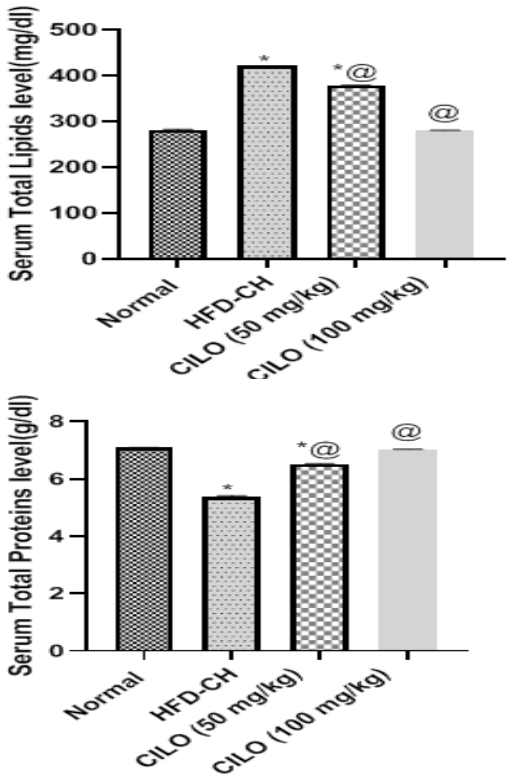

NAFLD was induced by daily administration of high fat diet rich in cholesterol for 10 weeks. Oral treatment of HFD-CH induced- NAFLD with CILO (50 and 100 mg/kg). 24 hours after the last dose of the drugs, fasting serum total lipids and total protein levels were evaluated. Results are expressed as mean ±SEM (n=8). *Significant difference from normal control group p< 0.05. @ Significant difference from NAFLD group.

Figure.2. Effect of cilostazol on fasting serum total lipids and total protein levels of NAFLD rats

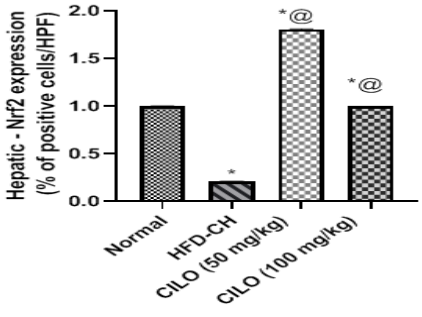

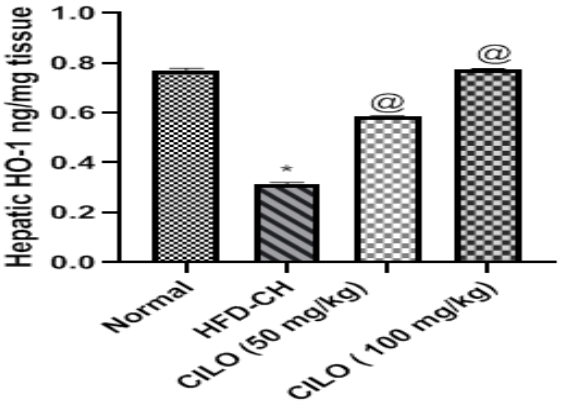

NAFLD was induced by daily administration of high fat diet rich in cholesterol for 10 weeks. Oral treatment of HFD-CH induced- NAFLD with CILO (50 and 100 mg/kg). 24 hours after the last dose of the drugs, hepatic Nrf-2 expression and HO-1 levels were evaluated. Results are expressed as mean ±SEM (n=8). *Significant difference from normal control group p< 0.05. @ Significant difference from NAFLD group.

Figure.3. Effect of cilostazol on Nrf-2 expression and HO-1 levels in hepatic tissue of NAFLD rats

Table.2.Effect of CILO on serum AST, ALT, ALP levels and hepatic concentration of TG_S and TC in NAFLD rats

Group / Parameter	Hepatic TNF-α level (pg/g tissue)	Hepatic NF-κB (pg/g tissue)
Normal	35.26±0.27	**18.67±0.15**
HFD-CH	128.5±0.2*	**84.76±0.23***
CILO(50 mg/kg)	65.07±0.02*@	**25.41±0.21*@**
CILO(100 mg/kg	32.46±0.64@	**18.83±0.27@**

.

Table.3.Effect of CILO on hepatic oxidative stress biomarkers in NAFLD rats

Group	Serum AST level (U/ml)	Serum ALT level (U/ml)	Serum ALP level (U/ml)	Hepatic TG_S (mg/g tissue)	Hepatic TC (mg/g tissue)
Normal	20.55±0.17	35.26±0.27	17.47±0.2	80±0.4	26.46±0.4
HFD-CH	126.5±0.2*	128.5±0.2*	108.5±0.12*	122.5±0.22*	62.34± 0.4*
CILO(50 mg/kg)	45.07±0.02*@	65.07±0.02*@	35.07±0.022*@	88.63±0.3*@	36.26± 0.16@
CILO(100 mg/kg	23.66±0.36*@	32.46±0.64*@	27.16±0.23*@	80.63±0.3@	25.60±0.44@

Table.4. Effect of CILO on hepatic levels of pro- inflammatory cytokines in NAFLD rats

Group / Parameter	Hepatic GSH level (nmol/g tissue)	Hepatic MDA level (nmol/g tissue)	Hepatic NO (nmol/g tissue)
Normal	32.55±0.19	90.66±0.17	**7.86±0.3**
HFD-CH	11.56±0.24*	226.5±0.2*	**45.9±0.005***
CILO (50 mg/kg)	36.29±0.27*@	98.07±0.02*@	**14.83±0.54*@**
CILO (100 mg/kg	33.99±0.4@	91.07±0.21@	**8.12±0.16@**

NAFLD was induced by daily administration of HFD-CH for 10 weeks. Oral treatment of HFD-CH induced- NAFLD with CILO (50 and 100 mg/kg). 24 hours after the last dose of the drugs, Hepatic levels of TNF-α and NF-κB were evaluated. Results are expressed as mean ±SEM (n=8). *Significant difference from normal control group p< 0.05. @ Significant difference from NAFLD group.

3.7. Effect of CILO on hepatic molecular alterations in NAFLD rats

Significant macromolecular bonding frequency regions are the characteristic features of the FT-IR spectra of hepatic specimens of HFD-CH. The most critical infrared absorbance bands are established between 1450 and 650 cm-1, amide I and II region between 1700 and 1500 cm-1, and C-H stretching region between 3070 and 2800 cm-1. Administration of CILO (100 mg/kg) for NAFLD rats succeeded to show corrected and normalized FTIR spectra **(Figure 4).**

3.8. Molecular docking study using MOE

Medicinal chemists faced problems and intricate challenges in the discovering of therapeutic compounds, so, docking is a highly demanding and efficient discipline in order to rationally develop compounds for treating human disease. In our study the potential of CILO as inhibitors for several biological targets including, peroxisome proliferator-activated receptor gamma (PPARγ), peroxisome proliferator-activated receptor alpha (PPARα), heme oxygenase-1 (HO1), transcription factor NF-E2-related factor 2 (Nrf2), tumor necrosis factor-alpha (TNF-α), glutathione reductase, inducible nitric oxide synthase (iNOS) and catalase, was investigated using molecular docking technology. The binding affinity and interaction manners of the cilostazol with the selected enzymes were depicted in **Table 1.** At the commencement, the native ligand for each enzyme was re-docked into the active pocket to validate our docking methodology, and the results showed that all re-docked ligands had a comparable conformation to the native ligands, with RMSD values ≤ 2.0 Å.

CILO revealed lower binding energy of -8.86 kcal/mol in the interaction with PPAR-γ (PDB ID: 3K8S), compared to the nativeligand, 2-chloro-N-{3-chloro-4-[(5-chloro-1,3-benzothiazol-2-yl)sulfanyl]phenyl}-4-(trifluoromethyl)benzenesulfonamide (**Z27**) with a docking energy of -9.94 kcal/mol (RMSD 1.94 Å, **Table 1**). Also, CILO showed excellent binding interaction with the PPAR-γ active site *via* formation two H-bonds donor, one H-bond acceptor and Three pi-H interaction with the key amino acids MET 348, GLN 286 and CYS 285, HIS 449, respectively in comparison to **Z27** which formed four H-bonds donor with MET 364 and CYS 285(**Table 1**, **Figure 5a&b**).

In the interaction with PPARα (PDB ID:3ET1, **Table 1**) , cilostazol formed two H-bonds acceptor with the amino acid TYR 334 (**Figure 6a&b**) and exhibited strong docking score of -9.39 kcal/mol compared to the native ligand 3-{5-methoxy-1-[(4-methoxyphenyl)sulfonyl]-1H-indol-3-yl}propanoic acid (**ET1**) with score -10.36 kcal/mol (RMSD 1.24 Å). Furthermore, docking of cilostazol with the HO1 enzyme (PDB ID: 1DVE) led to the establishment of two H-bonds acceptor and Pi-cation interaction with ASP 140 and ARG 136, with a docking score of -8.06 kcal/mol (**Table 1, Figure 7a&b)** compared to the native ligand, protoporphyrin IX containing Fe **(**HEM**)**of -11.82 kcal/mol (RMSD: 0.57Å). While, in the interaction with Nrf2 (PDB ID: 5CGJ), cilostazol, demonstrated a strong binding energy of -8.06 kcal/mol, which was lower than (3S)-1-(4-{[(2,3,5,6-tetramethylphenyl)sulfonyl]amino}naphthalen-1-yl)pyrrolidine-3-carboxylic acid (51M)of -7.32 kcal/mol (RMSD: 2.6 Å) with the formation of two H-bonds acceptor with the core amino acid ARG 483 (**Table 1, Figure 8a&b**).

In the instance of tumor necrosis factor-alpha (TNF-α; PDB ID: 2AZ5), CILO displayed good interaction with the enzyme active pocket by forming four H-bonds donor and two pi-H interaction with the key amino acids GLY 121 and LEU 55 (**Table 1, Figure 9a&b**). Additionally, cilostazol had lower docking score of -6.39 kcal/mol, compared to native ligand, 6,7-dimethyl-3-[(methyl{2-[methyl({1-[3-(trifluoromethyl)phenyl]-1H-indol-3-yl}methyl) amino]ethyl amino)methyl]-4H-chromen-4-one (307) of -7.74 kcal/mol (RMSD: 2Å). On the other hand, docking of cilostazol with glutathione reductase (PDB ID: 1XAN) showed better docking energy of -6.57 kcal/mol than co-crystalline ligand, 3,6-dihydroxy-xanthene-9-propionic acid **(**HXP) of -5.26 kcal/mol (RMSD: 2.5Å), with powerful interaction via formation of six H-bond acceptors with SER 470 and HIS 82 (**Table 1, Figure 10a&b**).

Interestingly, CILO displayed docking score of -7.60 kcal/mol with inducible nitric oxidesynthase (PDB ID: 4CX7) which very comparable to score of the co-crystalline ligand S71 [(R)-6-(3-amino-2-(5-(2-(6-amino-4-methylpyridin-2-yl)ethyl)pyridin-3-yl)propyl)-4-methylpyridin-2-amine], -7.95 kcal/mol and established a powerful interaction with the enzyme active pocket *via* formation of six H-donor, seven H-acceptor and five Pi-H bonds with the core amino acids MET 355, CYS 200, TYR 491, SER 242, GLY 371 and GLY 202 (**Table 1, Figure 11a&b**).

Finally, CILO stabilized itself in the catalase active pocket (PDB ID: 1TGU) through formation of three H-bonds acceptor and Three pi-pi interaction with ARG 364 and PHE 160and showed binding energy of -9.55 kcal/mol compared to co-crystalline ligand HEM of 14.85 and RMDS 0.46 Å (**Table 1**, **Figure 12a&b**).

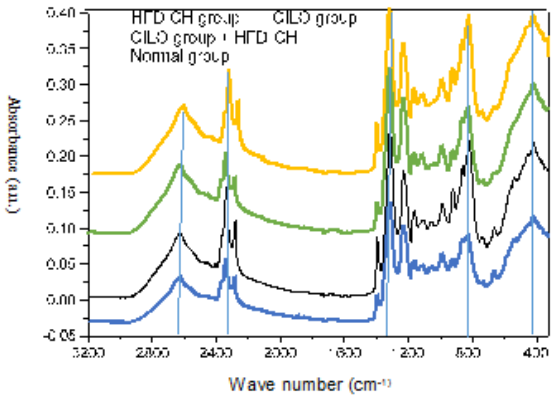

NAFLD was induced by daily administration of high fat diet rich in cholesterol for 10 weeks. Oral treatment of HFD-CH induced- NAFLD with CILO (50 and 100 mg/kg). 24 hours after the last dose of the drugs, wave number alterations were evaluated. Results are expressed as mean ±SEM (n=8). *Significant difference from normal control group $p < 0.05$. @ Significant difference from NAFLD group.

Figure.4. Effect of cilostazol on wave number alterations in hepatic tissue of NAFLD rats

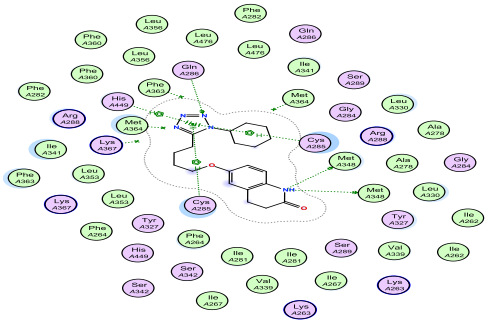

Figure 5a: 2D conformations of the **cilostazol** in the active site of the PPARγ receptor (PDB ID: 3K8S).

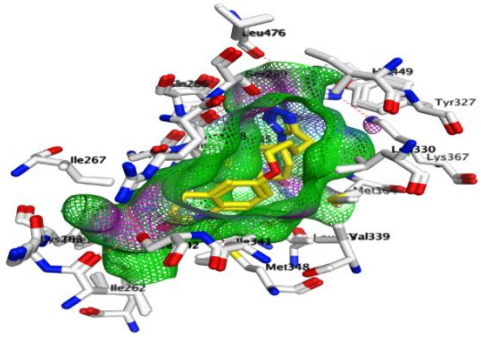

Figure 5b: 3D conformations of the **cilostazol** (yellow) in the active site of the PPARγ receptor (PDB ID: 3K8S).

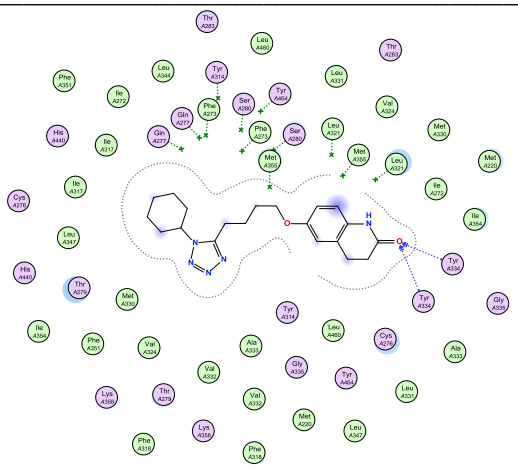

Figure 6a: 2D conformations of the **cilostazol** in the active site of the PPARα receptor (PDB ID: 3ET1).

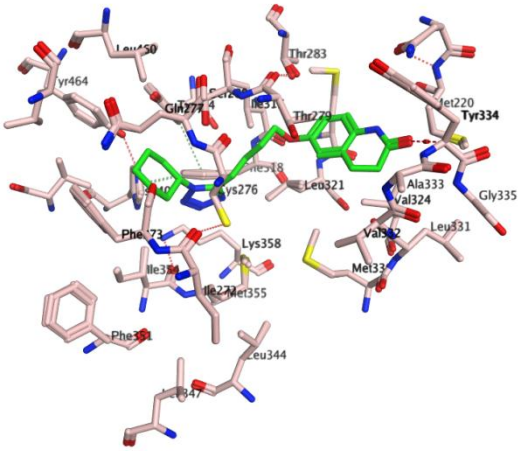

Figure 6b: 3D conformations of the **cilostazol** in the (green) active site of the PPARα receptor (PDB ID: 3ET1).

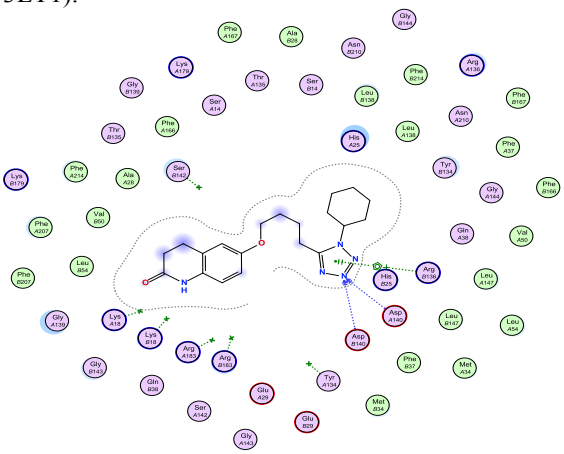

Figure 7a: 2D conformations of the **cilostazol** in the active site of the HO1 receptor (PDB ID: 1DVE).

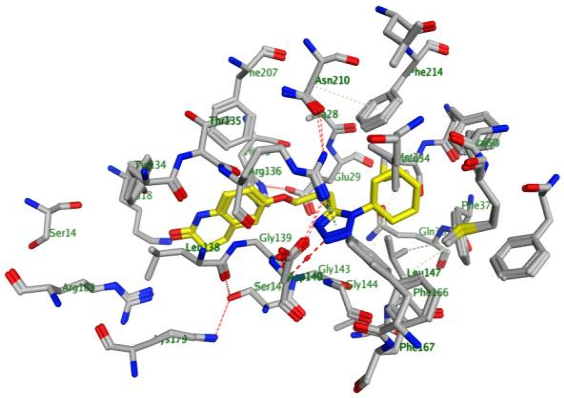

Figure 7b: 3D conformations of the **cilostazol** (yellow) in the active site of the HO1 receptor (PDB ID: 1DVE).

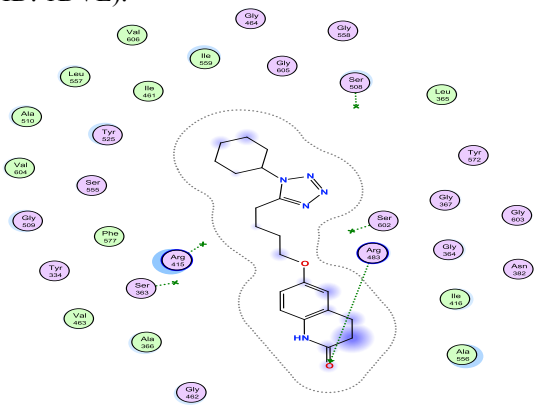

Figure 8a: 2D conformations of the **cilostazol** in the active site of the Nrf-2 receptor (PDB ID: 5CGJ).

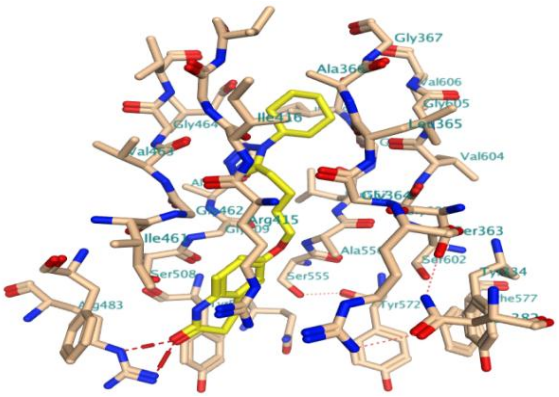

Figure 8b: 3D conformations of the **cilostazol** (yellow) in the active site of the Nrf-2 receptor (PDB ID: 5CGJ).

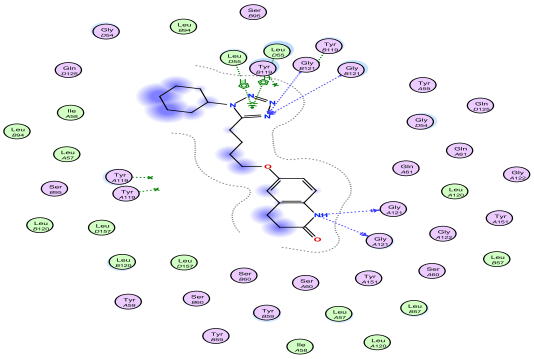

Figure 9a: 2D conformations of the **cilostazol** in the active site of the TNF-α receptor (PDB ID: 2AZ5).

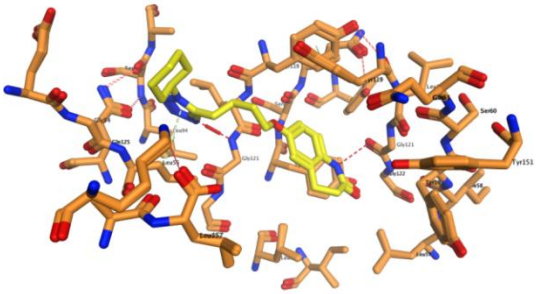

Figure 9b: 3D conformations of the **cilostazol** (yellow) in the active site of the TNF-α receptor (PDB ID: 2AZ5).

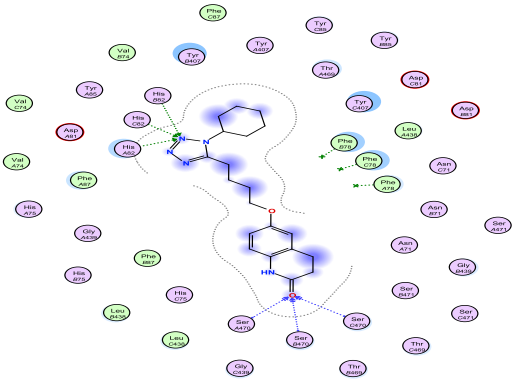

Figure 10a: 2D conformations of the **cilostazol** in the active site of the GSH receptor (PDB ID: 1XAN).

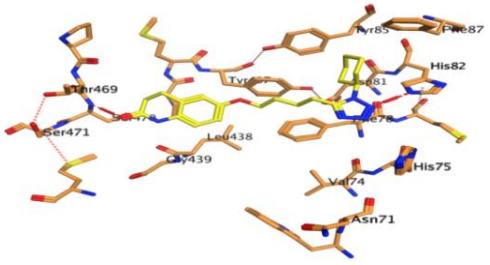

Figure 10b: 3D conformations of the **cilostazol** (yellow) in the active site of the GSH receptor (PDB ID: 1XAN)

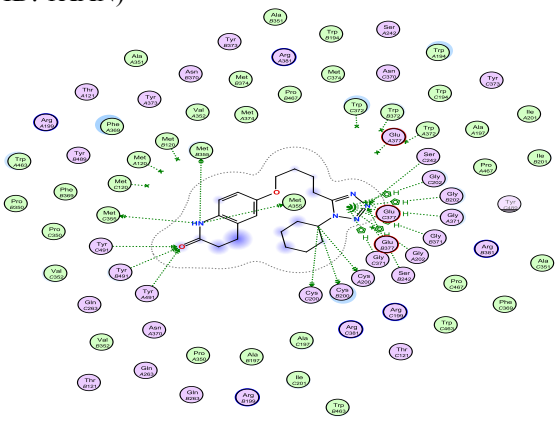

Figure 11a: 2D conformations of the **cilostazol** in the active site of the iNOS receptor (PDB ID: 4CX7).

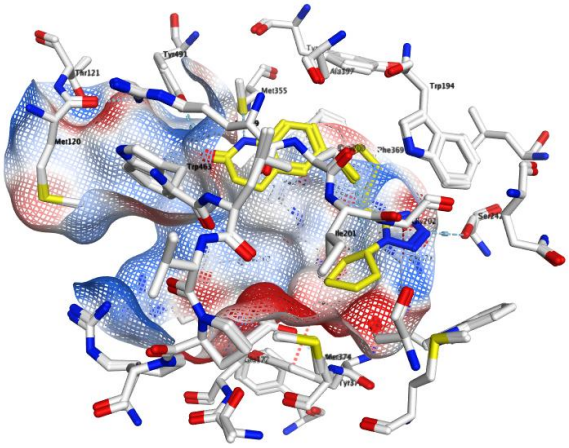

Figure 11b: 3D conformations of the **cilostazol** (yellow) in the active site of the iNOS receptor (PDB ID: 4CX7).

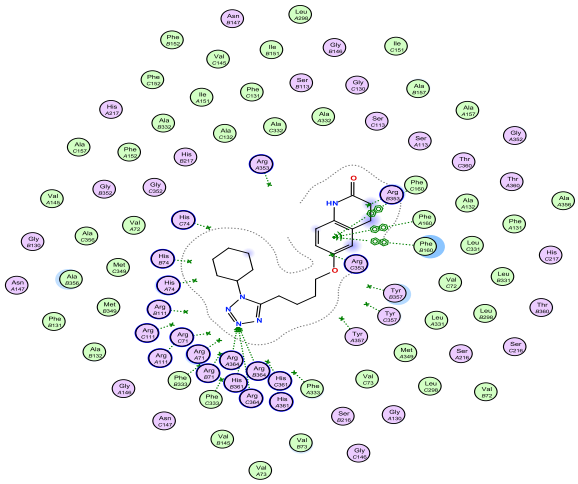

Figure 12a: 2D conformations of the **cilostazol** in the active site of the catalase receptor (PDB ID: 1TGU).

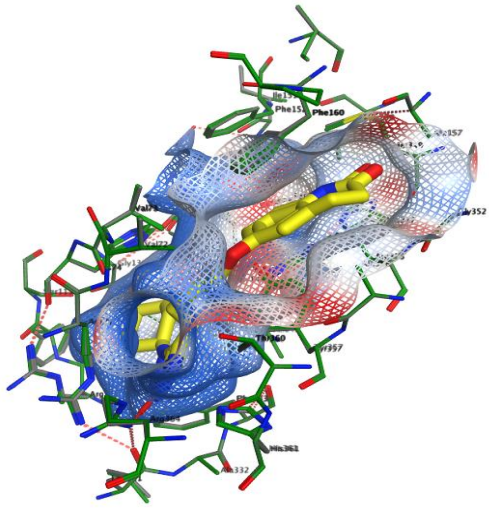

Figure 12b: 3D conformations of the **cilostazol** (yellow) in the active site of the catalase receptor (PDB ID: 1TGU).

4. Discussion

NAFLD (nonalcoholic fatty liver disease) is a hepato-metabolic disorder that is usually implicated in sever clinical and pathological disorders and is considered the major precipitating factors for insulin resistance, diabetes mellitus and cardiovascular diseases **(36)**. NAFLD is an asymptomatic hepatic manifestation that can lead to NASH, hepatic fibrosis, cirrhosis, and hepatic malignancy.**(37).**Weight loss regimen and exercise are the only accepted treatments but are often a challengeable matter for NAFLD patients. Thus, there is an urgent necessity to explore safe agents for reducing the elevated hepatic lipids. According to the authors' knowledge, this is the primary study exploring the valuable role of cilostazol, CILO; an Nrf2/HO-1 activator against the pathophysiological alterations induced by HFD- CH that parallel to NAFLD in human.

Excessive consumption of HFD-CH for 10 weeks was found to be a reliable and adequate model of NAFLD, displaying typical NAFLD symptoms such as obesity, decreased glucose tolerance, and hyperinsulinemea. In our study, HFD-CH was associated with increased glucose and insulin levels as a result of excess fat intake leads to hypertriglyceridemia and increased availability of free fatty acids which help in reducing the insulin-mediated drop in hepatic glucose production and decreases glucose uptake or utilization in skeletal muscle, resulting in hyperinsulinemia in our study

(38). Oral treatment of NAFLD with CILO (100 mg/kg) treatment for 10 weeks was associated with normalizing serum glucose and insulin levels due to CILO relaxing systemic arterioles, which may elevate blood flow through muscle tissue, thereby improving tissue response to glucose and insulin **(39)**.

Previous study indicated that the metabolic functions of CILO as a blood glucose disposal through its direct role in cellular glucose uptake by regulating glucose metabolizing enzymes, prostaglandin dehydrogenase and α-keto-glutarate dehydrogenase at the cellular membrane level **(40)**. Its well- known that the lipid composition of the erythrocyte membrane (EM)is affected by long term dietary fatty intake leading to accumulation of cholesterol within EM, alteration in phospholipid: cholesterol ratio, increase in the rigidity of EM and eventually increase the osmotic fragility of erythrocytes **(41)**.

Liver of rats received HFD-CH is frequently was associated with an extreme load of TGS, TC, and total lipids above the acceptable level, resulting in the liver's inability to metabolize free and bound lipids and a decrease in de novo synthesis of total proteins, resulting in a high concentration of TGS, TC, and total lipids in the free circulation and a decrease in total lipid concentration in the blood **(42)**. Our findings revealed that oral treatment of NAFLD rats with CILO (100 mg/kg) for 10 weeks was associated with normalization of TGS and TC hepatic concentrations **(43)**. NAFLD may be responsible for the induction of cellular hepatic enzymes AST, ALT, and ALP, which are used to assess liver function. AST and ALT are intracellular enzymes that serve as a clinical indicator of tissue injury, particularly hepatocyte tissue injury **(44)**. Serum ALT, AST, and ALP activity were shown to be elevated in HFD-CH-treated rats, indicating structural membrane disruption and the release of these enzymes into the systemic circulation. **(45)**. Oral administration of CILO (100 mg/kg) to NAFLD rats showed normalization in serum hepatic enzymes, demonstrating that CILO preserves the hepatocellular membrane's structural integrity **(46)**.

NAFLD has been associated with oxidative stress imbalance, with a general decrease in the efficiency of the antioxidant system expressed by exaggeration of ROS generation, increased lipid peroxidation in hepatocytes, and, as a result, impairment in redox homeostasis causes changes in pro-inflammatory cytokines **(47)**. Our results revealed that HFD-CH received rats have reduced levels of hepatic GSH levels and increased levels of lipid peroxidation products (MDA) **(48)**. There have been several biochemical routes and mechanisms of action proposed that link of generation of ROS with NAFLD, resulting in chronic oxidative stress. Other studies have found a large increase elevation in lipid peroxidation and a considerable reduction in hepatic antioxidant enzyme activities, which are consistent with the findings of this study **(49)**. In the current investigation, CILO was found to drastically alter the balance between oxidants and antioxidants in the livers of HFD-CH rats, resulting in a significant decrease in oxidative stress biomarkers and lipid peroxidation. CILO reduced hepatic lipid peroxidation and restored the activity of the GSH enzyme, which reduced oxidative stress by serving as an antioxidant and ROS scavenger. **(50)**. Exhaustion of glutathione in HFD-CH rats was related with a shift in oxidative stress indicators, which may debilitate cellular antioxidant defense to the point where NO produced by inducible NO synthase may cause hepatic damage **(51)**. Our promising study revealed that CILO could normalize the hepatic content of NO and these results are in consistent with **(52)**.

Hyperglycemia and elevated levels of free fatty acids and total lipids can triggers the release of proinflammatory cytokines and consequently hepatic inflammation as they are the driving forces for oxidative stress and ROS **(53)**.The initial induction of an early inflammatory response in response to NAFLD stimulates macrophages to produce cytokines, primarily, TNF-*α* and NF-κB **(54)**. TNF-*α,in particular, is involved in hepatic damage and is regarded as a critical sequela in various liver diseases* **(55)**. The finding of the present study showed that CILO could reduce the elevated levels of hepatic TNF-α and NF-κB. Our results are similar to a previous study reported that CILO could reduce the pro-inflammatory cytokines (TNF-α level) incommon bile duct ligated rats **(56)**. Moreover, CILO significantly reduced the expression of TNF-α mRNA and NF-κB from hepatocytes of rats received lipopolysaccharides **(57)** . As a result, our findings suggest that the hepatoprotective effects of CILO may be mediated by the suppression of the NF-κB system in rats received HFD-CH induced- NAFLD **(58)**.

Oxidative stress is regarded as one of the main precipitating factors associated with HFD-CH induced NAFLD. The transcription factor; Nrf2 protein participates effectively in triggering the induction of phase II detoxifying/antioxidant system

to cope with oxidative stress through enhancing the expression of a number of enzymes **(59)**. Under normal and oxidative stress conditions, redox balance is primarily regulated at the nuclear level, and Nrf2/HO-1 is an important mediator of such responses. As a result, in response to these stressful conditions, the expression of several genes has been upregulated for the defense against a wide range of diseases**(60)**. HO-1 is a stress-related protein that improves the rate-limiting step in heme degradation, which results in biliverdin, carbon monoxide, and free iron. where heme degradation products exhibit antioxidant activity and vasodilation, which can protect cells from oxidative stress **(61)**.The current study found that HFD-CH significantly reduced Nrf2 / HO-1 expression levels, which were improved by CILO, which played a protective role against oxidative insults by targeting Nrf2 / HO-1 induction **(62).**

FTIR spectroscopy was utilized to evaluate the hepatotoxic and hepatoprotective effects of numerous compounds, as well as biochemical changes in the liver, in a variety of animal models **(63)**. The current study examined molecular changes in liver tissue using the FTIR spectroscopy technique, in order to monitor the function group vibration modes present in proteins and lipids. FTIR spectra showed a broad characteristic peak at 3284 cm-1, which was attributed to a combination of O-H and N-H stretching vibrations. Also, an important peak was found at 2923 cm-1, it was attributed to the stretching vibration of the C-H2 group, that represented the lipids structure.**(63)**. The protein structure was represented by the peak at 1644 cm-1 which was a characteristic of N-H vibration (Amid I). Paying special attention to the range from 2923cm-1 to 3284 cm-1 typical of lipid C–H2 stretching, as well as the O–H vibrational stretching region 1644 cm-1 to 3284 cm-1 revealing that the wave number of fatty acid species changed significantly in NAFLD, indicating acyl chain modification of membrane lipids **(64).**

The buildup of lipids in the NAFLD group was indicated by FTIR analysis of the CH2, CH3 stretching area (3000–2800 cm1) and the ester carbonyl band at 1740 cm1**(65)**.A number of bands were fitted to the CH stretching region (3000–2800 cm1) to calculate the CH2/CH3 ratio. The decrease in the intensity of the CH_3 stretching modes, together with an increase in the CH_2 stretching modes, indicated that oxidative processes were occur in response to NAFLD and apoptosis is associated mainly with a change in the CH_2/CH_3 ratio **(66)**. Oral treatment of rats received HFD-CH with CILO could reduce the hepatic molecular alterations due to its effect as a non-enzymatic antioxidant and its ability to reduce hepatic lipids via Nrf2/Ho-1 activation **(67)**.

Regarding molecular docking analysis, this is the primary study involved in utilizing CILO biochemically and computationally as inhibitor for PPARγ, PPARα, HO-1, Nrf2, TNF-α, GSH, iNOS and catalase. The docking investigations were conducted using MOE 2019.01 (Molecular Operating Environment, Version 2019.01, Chemical Computing Group Inc., Montreal, Canada). The overall results indicated that CILO had excellent binding energy score and strong binding interactions with the core amino acids involved in the active pocket for the investigated enzymes **(Table 1)**.It is worthy to mention that, the tetrazole ring, NH and CO groups in CILO structure played a significant role in the binding interaction with the target enzymes as shown in **Table 1and Figures 6-12**.Our docking result indicated that, CILO had lower binding energy of -8.86 kcal/mol in the interaction with PPARγ (PDB ID: 3K8S) with the formation of three H-bonds and three pi-H interactions between NH group, tetrazole ring and MET 348, GLN 286, CYS 285, HIS 449 residues (**Table 1, Figure 5a&b**). While, molecular binding between CILO and PPARα (PDB ID:3ET1) active site have established two H-bonds acceptor between carbonyl group and TYR 334 residue with docking score of -9.39 kcal/mol (**Table 1, Figure 6a&b**). On the other hand, binding energy of CILO with HO-1 enzyme (PDB ID: 1DVE) was -8.06 kcal/mol and CILO - HO-1 complex was stabilized by establishment two H-bonds and Pi-cation interaction between tetrazole ring and ASP 140 and ARG 136 (**Table 1, Figure 7a&b**) . Interaction of cilostazol with Nrf2 (PDB ID: 5CGJ) resulted in low binding energy of -8.06kcal/mol, with good interaction with the active pockets through configuration of two H-bonds with the core amino acid ARG 483 and carbonyl group (**Table 1, Figure 8a&b**).

While, the complex produced by CILO and TNF- (PDB ID: 2AZ5) was stabilized by formation four H-bonds and two pi-H interactions between the NH group, tetrazole ring and the essential amino acids GLY 121 and LEU 55(**Table 1, Figure 9a&b**).Also, docking of CILO with glutathione reductase (PDB ID: 1XAN) revealed lower docking energy of -6.57 kcal/mol, with robust contact via formation of six H-bonds between tetrazole ring, carbonyl group, and SER 470, HIS 82 residues (**Table 1, Figure**

10a&b).The complex produced between CILO and inducible nitric oxide synthase (PDB ID: 4CX7) was shown to have a strong binding interaction, with thirteen H-bonds and five Pi-H bonds formed between the key amino acids MET 355, CYS 200, TYR 491, SER 242, GLY 371, GLY 202 and the NH, CO, cyclohexane, tetrazole rings (**Table 1, Figure 11a&b**).

Finally, docking of CILO with the catalase active pocket (PDB ID: 1TGU) demonstrated binding energy -9.55 kcal/mol and established three H-bonds and three pi-pi interaction with ARG 364 and PHE 160 (**Table 1, Figure 12a,b**).

Conclusions

Our findings revealed the possible modulatory role of cilostazol against high fat diet rich in cholesterol induced- NAFLD may be attributed to its anti-hyperlipedemic activity, activation of Nrf2/HO-1 pathway, reducing production of ROS and of pro-inflammatory mediators. Thus, CILO could be in used in the future for patients suffering from NAFLD. In addition to molecular docking proved that CILO had strong binding interactions with the core amino acids involved in the active pocket for each investigated enzymes and excellent binding energy score.

Declarations

Acknowledgments N/A

Funding N/A

Availability of data and materials: Available upon request

Author's information

Ahmed A. Sedik; Department of Pharmacology, Medical Research and Clinical Studies Institute, National Research Centre, Dokki, 12622, Cairo, Egypt

Asmaa A. Amer; Pharmacognosy Department, Pharmaceutical and Drug Industries Research Institute, National Research Centre, Dokki, 12622, Cairo, Egypt

Author Contributions

The authors declare that all data were generated in-house and that no paper mill was used. Ahmed A. Sedik has designed and conducted the study. Ahmed A.Sedik and Asmaa A.Amer shared in performing molecular docking studies. Authors had approved the latest version of the manuscript to be published.

Ethical Approval and consent to Participate

The study was approved by Medical Research Ethics Committee (MREC) of the National Research Centre (Egypt).

Competing interests

The authors declare that no conflict of interest.

5. References

1. Gupta A, Dhiman RK, Kumari S, Rana S, Agarwal R, Duseja A, et al. Role of small intestinal bacterial overgrowth and delayed gastrointestinal transit time in cirrhotic patients with minimal hepatic encephalopathy. 2010;53(5):849-55.
2. Targher GJDm. Non-alcoholic fatty liver disease, the metabolic syndrome and the risk of cardiovascular disease: the plot thickens. 2007;24(1):1-6.
3. Kanwar P, Nelson JE, Yates K, Kleiner DE, Unalp-Arida A, Kowdley KVJBog. Association between metabolic syndrome and liver histology among NAFLD patients without diabetes. 2016;3(1).
4. Al-Attar AM, Alrobai AA, Almalki DAJSjobs. Protective effect of olive and juniper leaves extracts on nephrotoxicity induced by thioacetamide in male mice. 2017;24(1):15-22.
5. Suzuki T, Yamamoto MJFRB, Medicine. Molecular basis of the Keap1–Nrf2 system. 2015;88:93-100.
6. Connolly MK, Bedrosian AS, Clair JM-S, Mitchell AP, Ibrahim J, Stroud A, et al. In liver fibrosis, dendritic cells govern hepatic inflammation in mice via TNF-α. 2009;119(11):3213-25.
7. David JA, Rifkin WJ, Rabbani PS, Ceradini DJJJodr. The Nrf2/Keap1/ARE pathway and oxidative stress as a therapeutic target in type II diabetes mellitus. 2017;2017.
8. Hernández A, Arab JP, Reyes D, Lapitz A, Moshage H, Bañales JM, et al. Extracellular Vesicles in NAFLD/ALD: From Pathobiology to Therapy. 2020;9(4):817.
9. Elam M, Heckman J, Crouse J, Hunninghake D, Herd J, Davidson M, et al. Effect of the novel antiplatelet agent cilostazol on plasma lipoproteins in patients with intermittent claudication. 1998;18(12):1942-7.
10. Balinski AM, Preuss CV. Cilostazol. 2019.
11. Chen Y, Pandiri I, Joe Y, Kim HJ, Kim S-K, Park J, et al. Synergistic effects of cilostazol and probucol on ER stress-induced hepatic steatosis via heme oxygenase-1-dependent activation of mitochondrial biogenesis. 2016;2016.

12. Nazar MF, Abdullah MI, Badshah A, Mahmood A, Rana UA, Khan SU-D. Synthesis, structure–activity relationship and molecular docking of cyclohexenone based analogous as potent non-nucleoside reverse-transcriptase inhibitors. Journal of Molecular Structure. 2015;1086:8-16.
13. Ahmad F, Mahmood A, Muhmood T. Machine learning-integrated omics for the risk and safety assessment of nanomaterials. Biomaterials science. 2021.
14. Ramadan AA, Afifi NA, Erian EY, Saleh DO, Sedik AAJWJPPS. Beneficial effect of trigonelline on the metabolic changes associated with insulin resistance in rats. 2015;5(2):1238-50.
15. El Awdan SA, Abdel Rahman RF, Ibrahim HM, Hegazy RR, El Marasy SA, Badawi M, et al. Regression of fibrosis by cilostazol in a rat model of thioacetamide-induced liver fibrosis: Up regulation of hepatic cAMP, and modulation of inflammatory, oxidative stress and apoptotic biomarkers. 2019;14(5):e0216301.
16. Trinder PJJocp. Determination of blood glucose using an oxidase-peroxidase system with a non-carcinogenic chromogen. 1969;22(2):158-61.
17. Grassi J, Roberge CJ, Frobert Y, Pradelles P, Poubelle PEJIr. Determination of ILlα, ILlβ and IL2 in Biological Media using Specific Enzyme Immunometric Assays. 1991;119(1):125-45.
18. Reitman S, Frankel SJAjocp. A colorimetric method for the determination of serum glutamic oxalacetic and glutamic pyruvic transaminases. 1957;28(1):56-63.
19. Richmond WJCc. Preparation and properties of a cholesterol oxidase from Nocardia sp. and its application to the enzymatic assay of total cholesterol in serum. 1973;19(12):1350-6.
20. Fassati P, Principe LJCC. Measurement of serum triglyceride colorimetrically with an enzyme that produce H2O2. 1982;28(10):2077-80.
21. Evans J, Ellman GJBeBA. The ionization of cysteine. 1959;33(2):574-6.
22. Ohkawa H, Ohishi N, Yagi KJAb. Assay for lipid peroxides in animal tissues by thiobarbituric acid reaction. 1979;95(2):351-8.
23. Ridnour LA, Sim JE, Hayward MA, Wink DA, Martin SM, Buettner GR, et al. A spectrophotometric method for the direct detection and quantitation of nitric oxide, nitrite, and nitrate in cell culture media. 2000;281(2):223-9.
24. Marklund S, Marklund GJEjob. Involvement of the superoxide anion radical in the autoxidation of pyrogallol and a convenient assay for superoxide dismutase. 1974;47(3):469-74.
25. Marrazzo G, Bosco P, La Delia F, Scapagnini G, Di Giacomo C, Malaguarnera M, et al. Neuroprotective effect of silibinin in diabetic mice. 2011;504(3):252-6.
26. Severcan F, Toyran N, Kaptan N, Turan BJT. Fourier transform infrared study of the effect of diabetes on rat liver and heart tissues in the C□H region. 2000;53(1):55-9.
27. Sivakumar S, Sivasubramanian J, Raja BJSAPAM, Spectroscopy B. Aluminium induced structural, metabolic alterations and protective effects of desferrioxamine in the brain tissue of mice: an FTIR study. 2012;99:252-8.
28. Li Y, Wang Z, Furukawa N, Escaron P, Weiszmann J, Lee G, et al. T2384, a novel antidiabetic agent with unique peroxisome proliferator-activated receptor γ binding properties. Journal of Biological Chemistry. 2008;283(14):9168-76.
29. Artis DR, Lin JJ, Zhang C, Wang W, Mehra U, Perreault M, et al. Scaffold-based discovery of indeglitazar, a PPAR pan-active anti-diabetic agent. Proceedings of the National Academy of Sciences. 2009;106(1):262-7.
30. Sugishima M, Omata Y, Kakuta Y, Sakamoto H, Noguchi M, Fukuyama K. Crystal structure of rat heme oxygenase-1 in complex with heme. FEBS letters. 2000;471(1):61-6.
31. Winkel AF, Engel CK, Margerie D, Kannt A, Szillat H, Glombik H, et al. Characterization of RA839, a noncovalent small molecule binder to Keap1 and selective activator of Nrf2 signaling. Journal of Biological Chemistry. 2015;290(47):28446-55.
32. He MM, Smith AS, Oslob JD, Flanagan WM, Braisted AC, Whitty A, et al. Small-molecule inhibition of TNF-α. Science. 2005;310(5750):1022-5.
33. Savvides SN, Karplus PA. Kinetics and crystallographic analysis of human glutathione reductase in complex with a xanthene inhibitor. Journal of Biological Chemistry. 1996;271(14):8101-7.
34. Li H, Jamal J, Delker S, Plaza C, Ji H, Jing Q, et al. The mobility of a conserved tyrosine residue controls isoform-dependent enzyme–inhibitor interactions in nitric oxide synthases. Biochemistry. 2014;53(32):5272-9.
35. Gouet P, Jouve H-M, Dideberg O. Crystal Structure ofProteus mirabilisPR Catalase With

and Without Bound NADPH. Journal of molecular biology. 1995;249(5):933-54.
36. Buzzetti E, Pinzani M, Tsochatzis EAJM. The multiple-hit pathogenesis of non-alcoholic fatty liver disease (NAFLD). 2016;65(8):1038-48.
37. Wang MQ, Yan AF, Katz RV. Annals of Internal Medicine Researcher Requests for Inappropriate Analysis and Reporting: AU. S. Survey of Consulting Biostatisticians.
38. Flock MR, Green MH, Kris-Etherton PMJAiN. Effects of adiposity on plasma lipid response to reductions in dietary saturated fatty acids and cholesterol. 2011;2(3):261-74.
39. Chang SA, Cha BY, Yoo SJ, Ahn YB, Song KH, Han JH, et al. The effect of cilostazol on glucose tolerance and insulin resistance in a rat model of non-insulin dependent diabetes mellitus. The Korean journal of internal medicine. 2001;16(2):87.
40. Grunwald P. Enzyme Kinetics and Drugs as Enzyme Inhibitors. Pharmaceutical Biocatalysis: Jenny Stanford Publishing; 2019. p. 721-806.
41. Perona JS. Membrane lipid alterations in the metabolic syndrome and the role of dietary oils. Elsevier; 2017.
42. Heeba GH, El-Deen R, Abdel-latif RG, Khalifa MMAJCJoP, Pharmacology. Combined treatments with metformin and phosphodiesterase inhibitors alleviate non-alcoholic fatty liver disease in high-fat diet-fed rats: A comparative study. 2020(ja).
43. Park J-h, Choi B-h, Ku S-K, Kim D-h, Jung K-A, Oh E, et al. Amelioration of high fat diet-induced nephropathy by cilostazol and rosuvastatin. Archives of pharmacal research. 2017;40(3):391-402.
44. Smith BW, Adams LA. Non-alcoholic fatty liver disease. Critical reviews in clinical laboratory sciences. 2011;48(3):97-113.
45. Harris E, Macpherson H, Pipingas AJN. Improved blood biomarkers but no cognitive effects from 16 weeks of multivitamin supplementation in healthy older adults. 2015;7(5):3796-812.
46. Kabil SL. Beneficial effects of cilostazol on liver injury induced by common bile duct ligation in rats: role of SIRT 1 signaling pathway. Clinical and Experimental Pharmacology and Physiology. 2018;45(12):1341-50.
47. Afifi NA, Ramadan A, Erian EY, Saleh DO, Sedik AA, Badawi M, et al. Trigonelline attenuates hepatic complications and molecular alterations in high-fat high-fructose diet-induced insulin resistance in rats. 2017;95(4):427-36.
48. Reddy PVB, Murthy CR, Reddanna PJNl. Fulminant hepatic failure induced oxidative stress in nonsynaptic mitochondria of cerebral cortex in rats. 2004;368(1):15-20.
49. Nandhini A, Thirunavukkarasu V, Ravichandran M, Anuradha CJSmj. Effect of taurine on biomarkers of oxidative stress in tissues of fructose-fed insulin-resistant rats. 2005;46(2):82.
50. Ragab D, Abdallah DM, El-Abhar HSJPo. Cilostazol renoprotective effect: Modulation of PPAR-γ, NGAL, KIM-1 and IL-18 underlies its novel effect in a model of ischemia-reperfusion. 2014;9(5):e95313.
51. Bartesaghi S, Radi RJRb. Fundamentals on the biochemistry of peroxynitrite and protein tyrosine nitration. 2018;14:618-25.
52. Abdelsameea AA, Mohamed AM, Amer MG, Attia SMJE, Pathology T. Cilostazol attenuates gentamicin-induced nephrotoxicity in rats. 2016;68(4):247-53.
53. Llacuna L, Bárcena C, Bellido-Martín L, Fernández L, Stefanovic M, Marí M, et al. Growth arrest–specific protein 6 is hepatoprotective against murine ischemia/reperfusion injury. 2010;52(4):1371-9.
54. Diao Y, Zhao X-F, Lin J-S, Wang Q-Z, Xu R-AJWJoGW. Protection of the liver against CCl4-induced injury by intramuscular electrotransfer of a kallistatin-encoding plasmid. 2011;17(1):111.
55. Auguet T, Vidal F, López-Dupla M, Broch M, Gutiérrez C, Olona M, et al. A study on the TNF-α system in Caucasian Spanish patients with alcoholic liver disease. 2008;92(1-3):91-9.
56. Kawy HSAJEJoP. Cilostazol attenuates cholestatic liver injury and its complications in common bile duct ligated rats. 2015;752:8-17.
57. Lee D-E, Koo H, Sun I-C, Ryu JH, Kim K, Kwon ICJCSR. Multifunctional nanoparticles for multimodal imaging and theragnosis. 2012;41(7):2656-72.
58. da Motta NAV, de Brito FCF. Cilostazol exerts antiplatelet and anti-inflammatory effects through AMPK activation and NF-kB inhibition on hypercholesterolemic rats. Fundamental & clinical pharmacology. 2016;30(4):327-37.
59. Orhan C, Akdemir F, Sahin N, Tuzcu M, Komorowski J, Hayirli A, et al. Chromium histidinate protects against heat stress by

modulating the expression of hepatic nuclear transcription factors in quail. 2012;53(6):828-35.
60. Kim HJ, Moon JH, Kim HM, Yun MR, Jeon BH, Lee B, et al. The hypolipidemic effect of cilostazol can be mediated by regulation of hepatic low-density lipoprotein receptor-related protein 1 (LRP1) expression. 2014;63(1):112-9.
61. Lawal AO, Ellis EMJEt, pharmacology. Nrf2-mediated adaptive response to cadmium-induced toxicity involves protein kinase C delta in human 1321N1 astrocytoma cells. 2011;32(1):54-62.
62. Abuelezz SA, Hendawy NJBP. Insights into the potential antidepressant mechanisms of cilostazol in chronically restraint rats: impact on the Nrf2 pathway. 2018;29(1):28-40.
63. Liyanage S, Abidi N. Fourier transform infrared applications to investigate induced biochemical changes in liver. Applied Spectroscopy Reviews. 2020;55(9-10):840-72.
64. Baquet ZC, Gorski JA, Jones KRJJoN. Early striatal dendrite deficits followed by neuron loss with advanced age in the absence of anterograde cortical brain-derived neurotrophic factor. 2004;24(17):4250-8.
65. Gupta RK, Swain SR, Sahoo J, Chaudhary S, Gupta A. Isolation, characterization and hepatoprotective activity of naturally occurring protopine against simvastatin induced liver toxicity in experimental rodents. Current Bioactive Compounds. 2020;16(5):568-75.
66. Blankenberg FG, Katsikis PD, Storrs RW, Beaulieu C, Spielman D, Chen JY, et al. Quantitative analysis of apoptotic cell death using proton nuclear magnetic resonance spectroscopy. 1997;89(10):3778-86.
67. Park SY, Lee SW, Baek SH, Lee SJ, Lee WS, Rhim BY, et al. Induction of heme oxygenase-1 expression by cilostazol contributes to its anti-inflammatory effects in J774 murine macrophages. Immunology letters. 2011;136(2):138-45.